The Lurcher Mutation Identifies $\delta 2$ as an AMPA/Kainate Receptor-Like Channel That Is Potentiated by Ca^{2+}

Lonnie P. Wollmuth,[1] Thomas Kuner,[2,3] Claudia Jatzke,[1] Peter H. Seeburg,[3] Nathaniel Heintz,[4] and Jian Zuo[4,5]

[1]*Department of Neurobiology and Behavior, State University of New York at Stony Brook, Stony Brook, New York 11794-5230,* [2]*Department of Neurobiology, Duke University Medical Center, Durham, North Carolina 27710,* [3]*Abteilung Molekulare Neurobiologie, Max-Planck-Institut für medizinische Forschung, D-69120 Heidelberg, Germany,* [4]*Laboratory of Molecular Biology, Howard Hughes Medical Institute, The Rockefeller University, New York, New York 10021, and* [5]*Department of Developmental Neurobiology, St. Jude Children's Research Hospital, Memphis, Tennessee 38105*

Neurodegeneration in Lurcher (*Lc*) mice results from constitutive activation of $\delta 2$, a subunit of ionotropic glutamate receptors (GluRs) with unknown natural ligands and channel properties. Homo-oligomeric channels of GluR-$\delta 2$ with the Lurcher mutation (GluR-$\delta 2^{Lc}$) expressed in human embryonic kidney 293 cells showed a doubly rectifying current–voltage relation reminiscent of the block by intracellular polyamines in AMPA/kainate channels. Similarly, the fraction of the total current carried by Ca^{2+} was ~2–3%, comparable with that found in Ca^{2+}-permeable AMPA/kainate channels. Currents through GluR-$\delta 2^{Lc}$ channels were also potentiated by extracellular Ca^{2+} in a biphasic manner, with maximal potentiation occurring at physiological concentrations of Ca^{2+}. We examined the functional role of the Q/R site in GluR-$\delta 2^{Lc}$ by replacing glutamine with arginine. Analogous to AMPA/kainate receptors, GluR-$\delta 2^{Lc}$(R) channels showed no voltage-dependent block by intracellular polyamines and were nominally impermeable to Ca^{2+}. The potentiation by Ca^{2+}, however, remained intact. Hence, GluR-$\delta 2^{Lc}$ channels are functionally similar to the AMPA/kainate receptor channels, consistent with the high-sequence identity shared by these subunits within the channel-lining M2 and M3 segments. Furthermore, potentiation by Ca^{2+} and a permeability to Ca^{2+} comparable with that of AMPA/kainate receptors provide a possible cause for cell death in Lurcher mice and may contribute to cerebellar long-term depression under physiological conditions.

Key words: glutamate receptors; $\delta 2$; Lurcher mutation; polyamine block; Ca^{2+} permeability; fractional Ca^{2+} currents

---

$\delta 1$ and $\delta 2$ are members of the ionotropic glutamate receptor (GluR) family, sharing ~20–30% sequence identity with NMDA and AMPA/kainate receptor subunits (Yamazaki et al., 1992; Araki et al., 1993; Lomeli et al., 1993). They differ from other members, however, in that they neither bind nor are activated by glutamate or other typical GluR agonists. Members of the δ subfamily therefore have been classified as "orphan" glutamate receptors.

GluR-$\delta 2$ shows a restricted distribution, occurring predominantly in cerebellar Purkinje neurons (Araki et al., 1993; Lomeli et al., 1993). This distribution is further restricted primarily to the parallel fiber→Purkinje neuron synapse (Landsend et al., 1997; Zhao et al., 1997). Although the cellular function of GluR-$\delta 2$ is unknown, mice lacking it show motor coordination deficits, abnormal synapse formation in the cerebellum (climbing fiber→Purkinje neuron and parallel fiber→Purkinje neuron), and impaired long-term depression at the parallel fiber→Purkinje neuron synapse (Kashiwabuchi et al., 1995). In addition, Lurcher (*Lc*) is a semi-dominant neurological mutation with heterozygous Lurcher mice (*Lc*/+) displaying ataxia because of a selective loss of cerebellar Purkinje neurons during postnatal development (for review, see Heintz and De Jager, 1999). Neurodegeneration in Lurcher mice arises from a single

amino acid substitution (alanine to threonine) in the highly conserved third hydrophobic segment (M3) of the GluR-$\delta 2$ protein (Zuo et al., 1997) (see Fig. 1). This mutation, termed the Lurcher mutation, results in channels that are constitutively open. Indeed, in *Lc*/+ mice, Purkinje neurons display a high membrane conductance and a depolarized resting membrane potential. Similarly, heterologous expression of GluR-$\delta 2$ with the Lurcher mutation (GluR-$\delta 2^{Lc}$) in *Xenopus* oocytes confirms that the Lurcher mutation results in channels that are constitutively active (Zuo et al., 1997).
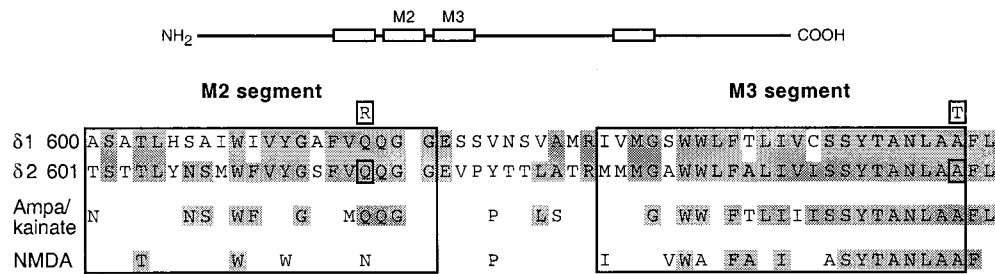
The mechanism by which the Lurcher mutation induces cell death in the cerebellum is unknown (Heintz and De Jager, 1999). In part, this reflects that the basic properties of the channel formed by GluR-$\delta 2^{Lc}$ have not been characterized. To understand further how the Lurcher mutation induces cell death and to gain insight into the cellular function of GluR-$\delta 2$, we investigated the permeation properties of homo-oligomeric GluR-$\delta 2^{Lc}$ channels. Figure 1 compares the primary structure of the M2 and M3 domains in GluR subtypes. Although not exclusively, the M2 and M3 segments form the central core of the ion conduction pathway in NMDA and AMPA/kainate receptor channels (Kuner et al., 1999). Within this core region, GluR-$\delta 2$ shows a much higher sequence identity to AMPA/kainate than to NMDA receptors. In addition, the amino acid residue occupying the functionally critical Q/R/N site strongly influences the permeation properties of GluR channels (see Burnashev, 1996). In wild-type GluR-$\delta 2$, this site is occupied by a glutamine (Q), as in Ca^{2+}-permeable AMPA/kainate receptor channels. We therefore constructed a Lurcher channel with the positively charged arginine (R) substituted at this position. In agreement with the sequence similarity, we find that GluR-$\delta 2^{Lc}$ forms channels with properties comparable with those of Ca^{2+}-permeable AMPA/kainate channels. In addition, and in contrast to other GluR subtypes, current through Lurcher channels is strongly potentiated by extracellular Ca^{2+}.

Figure 1. Sequence alignment of the M2 and M3 segments in glutamate receptor subtypes. *Top*, Schematic drawing of GluR subunits with the four hydrophobic segments (M1–M4) indicated as *open boxes*. *Bottom*, Enlarged region showing a sequence alignment of the *M2* and *M3* amino acid residues of the GluR-δ1 and -δ2 subunits and of the consensus sequence for AMPA/kainate and NMDA subtypes. The gaps in the sequences for AMPA/kainate and NMDA subtypes indicate positions that are occupied by nonidentical amino acid residues across members of the indicated receptor family. The AMPA/kainate consensus sequence is based on AMPA (GluR-A, -B, -C, and -D) and low (GluR-5, -6, and -7) and high (KA-1 and -2) affinity kainate receptors. The GluR-B subunit was used in its unedited form. The NMDA consensus sequence is based on the NR1 and all NR2 (A–D) subunits. For GluR-δ1 and -δ2, the *sequence numbers* (*left*) are for the mature protein. The *shaded residues* indicate those shared by at least two sequences using GluR-δ2 as the reference. Over this region and relative to GluR-δ2, GluR-δ1 shows 63% identity, and AMPA/kainate and NMDA sequences show 48 and 25% identity, respectively. Sequence identity for the whole protein is less (δ1, 53%; AMPA/kainate, 24–28%; and NMDA, 19–23%). *Boxed amino acids* depict mutations of δ2 used in the present study. The alanine (*A*) to threonine (*T*) substitution at position 654 is the Lurcher mutation, and channels containing it were identified as GluR-δ2^{Lc}(Q). Within the Lurcher background, a second substitution, the positively charged arginine (*R*) for glutamine (*Q*) at position 618, was also made [GluR-δ2^{Lc}(R)].

MATERIALS AND METHODS

Molecular biology

AMPA receptor (AMPAR) subunits were identified following the nomenclature of Seeburg (1993), with the amino acid residue occupying the Q/R site indicated in parenthesis.

Wild-type GluR-δ2(Q) construct

A full-length cDNA clone was isolated from a cerebellar cDNA library of postnatal day 12 wild-type mice. PCR amplification using the expanded high-fidelity PCR amplification system was used to introduce a biochemical tag [hemagglutinin 1 (HA1)], T7 primer, and other necessary transcriptional elements. Two primers were designed on the basis of the mouse GluR-δ2 cDNA sequences (D13266): GluR-δ2-1 (5′-CCAAGCTTCTAA-TACGACTCACTATAGGGTTTTTATTTTTTAATTTTCTTTCAAAT-ACTTCCACCATGGAAGTTTTCCCCTTGCTC-3′) consists of a leader sequence (9 base pairs), a T7 primer sequence (17 base pairs), untranslated leader (37 base pairs) sequence, and 5′ GluR-δ2-coding sequence (21 base pairs from the ATG initiation start site); and GluR-δ2-2 (5′-TTTTT TTTTTTTTTTTTTTTTTCAAGCATAATCAGGAACATCATAAG-GA TATATGG ACGTGCCTCGGTCGG-3′) consists of the 3′-coding region of GluR-δ2 (20 base pairs ending before the stop codon ATA), an HA tag (27 base pairs encoding the YPYDVPDYA epitope), a TGA stop codon, and 20 polyAs. PCR products were cloned into pCR3.1, the bidirectional eukaryotic TA-cloning vector (Invitrogen, Carlsbad, CA). The entire cDNA clone was subsequently verified by sequencing using primers corresponding to the coding sequences of mouse GluR-δ2 (D13266).

Mutant GluR-δ2^{Lc}(Q) and GluR-δ2^{Lc}(R) constructs

We used the bridge PCR mutagenesis method (Ho et al., 1989) to introduce point mutations in the GluR-δ2(Q) construct. Two oligonucleotides were designed to create the GluR-δ2^{Lc}(Q) construct: GluR-δ2-m1 (5′-CCAACCTTGCCACTTTCCTCAC-3′) and GluR-δ2-m2 (complementary to GluR-δ2-m1). Two additional oligonucleotides were designed for the GluR-δ2^{Lc}(R) construct: GluR-δ2-Q618R-1 (5′-GGATCCTTTGTAAG-GCAAGGTGGG-3′) and GluR-δ2-Q618R-2 (complementary to GluR-δ2-Q618R-1). The wild-type GluR-δ2(Q) construct was digested using *Bgl*II and *Sac*II to release the fragment from 1149 to 2519 of the coding sequence. Two other oligonucleotides were designed for subcloning purposes: GluR-δ2-F1139 with the *Bgl*II site (5′-TAGTCCGAATTCGAT-TGACTGGAGACTAG-3′) and GluR-δ2-R2532 with the *Sac*II site (5′-GAGCACAATTCCCGCGGCCAGG-3′).

Briefly, to create GluR-δ2^{Lc}(Q), GluR-δ2-F1139 and GluR-δ2-m2, along with GluR-δ2(Q)-m1 and GluR-δ2-R2532, were used for amplification from the wild-type cDNA clone GluR-δ2(Q). Two PCR products were then mixed for further amplification using the two outside primers GluR-δ2-F1139 and GluR-δ2-R2532. The final PCR product was digested with *Bgl*II and *Sac*II for subcloning into the GluR-δ2(Q) wild-type clone. A similar strategy was used for creating the GluR-δ2^{Lc}(R) clone. Both clones were verified by restriction digests and sequencing.

In vitro *translation of GluR-δ2(Q) and GluR-δ2^{Lc}(Q) constructs*

To confirm that the constructs lead to the expected protein products, we performed an *in vitro* translation assay using the T7-coupled reticulate lysate system with [^{35}S]methionine (Promega, Madison, WI). Both GluR-δ2(Q) and GluR-δ2^{Lc}(Q) resulted in protein products of 110 kDa analyzed in 7.5% SDS-PAGE gels (data not shown).

Heterologous expression of GluR-δ2(Q), GluR-δ2^{Lc}(Q), and GluR-δ2^{Lc}(R)

Human embryonic kidney 293 cells (HEK 293) were transiently transfected with expression vectors for GluR-δ2(Q), GluR-δ2^{Lc}(Q), and GluR-δ2^{Lc}(R). To detect transfected cells, a vector for green fluorescent protein (GFP) was cotransfected at a ratio of 1:6. Whole-cell recordings were made 2 d after transfection. We assumed that cells fluorescent for GFP were also expressing GluR-δ2(Q), GluR-δ2^{Lc}(Q), or GluR-δ2^{Lc}(R) because previous experience with glutamate-activated GluR subtypes showed that coexpression occurred >95% of the time.

Solutions

Intracellular

Our standard intracellular solution consisted of (in mM): 140 CsCl, 10 HEPES, and 1 BAPTA (or 1 fura-2), with the pH adjusted to 7.2 with CsOH. In some instances, the BAPTA concentration was decreased (to 0.1 mM) or increased (to 10 mM). To measure changes in intracellular Ca^{2+}, we replaced BAPTA with 1 mM fura-2 (K$_5$·fura-2). HEPES and BAPTA were obtained from Sigma (St. Louis, MO), and fura-2 was from Molecular Probes (Eugene, OR).

Extracellular

Our standard extracellular solution, based on normal rat Ringer's solution, consisted of (in mM): 135 NaCl, 5.4 KCl, 0.5 MgCl$_2$, and 5 HEPES, with the pH adjusted to 7.2 using NaOH. We refer to this solution as the "high-Na$^+$" solution. In a few experiments, Mg^{2+} was omitted from this solution. The *N*-methyl-D-glucamine (NMDG) solution consisted of (in mM): 140 NMDG, 0.5 MgCl$_2$, and 5 HEPES. All divalent cations tested were added without substitutions to the high-Na$^+$ or NMDG solutions. NMDG was obtained from Sigma.

Current recordings and data analysis

Currents were recorded at room temperature (20–23°C) using an EPC-7 or EPC-9 amplifier with PULSE software (HEKA Elektronik, Lambrecht, Germany), low-pass filtered at 500 Hz, and digitized at 2 kHz. Pipettes were pulled from borosilicate glass and had resistances of 1–4 MΩ when filled with the pipette solution and measured in the high-Na$^+$ extracellular solution. External solutions were applied using a piezo-driven double-barrel application system (see Wollmuth et al., 1996). In our standard experimental protocol, one barrel contained the high-Na$^+$ solution (control solution), and the other barrel contained the same solution but with added divalents (test solution). In most instances, voltage ramps (~120 mV·sec^{-1}) were used to determine the potential dependence of currents. Voltage ramps in the control solution were always made before and after application of the test solution. To quantify zero-current (reversal) potentials (V_{rev}), we fitted a third-order polynomial to current records. The standard definition of chord conductance (G) was used: $G = I_{amp}/(V_m - V_{rev})$, where I_{amp} is the current amplitude at the membrane potential V_m. All curve fitting was done using Igor Pro (WaveMetrics, Lake Oswego, OR). Results are reported in the text as the mean ± SEM and shown graphically as the mean ± 2 * SEM. An ANOVA was used to test for statistical differences in current amplitudes (see Fig. 2*B*), conductances (see Figs. 2*C*, 3*B*), and fractional Ca^{2+} currents (see Fig. 7). The Tukey

test was used for multiple comparisons. Unless otherwise noted, significance was assumed if $p < 0.05$.

Fractional Ca^{2+} currents

Fura-2 (1 mM) was loaded into HEK 293 cells via the patch pipette to measure the fraction of the total current (monovalents and Ca^{2+}) carried by Ca^{2+} (Neher, 1995; for additional details, see Wollmuth and Sakmann, 1998). Briefly, cells were illuminated alternatively at 360 and 380 nm (2–10 Hz) by a polychromatic illumination system (T.I.L.L. Photonics, München, Germany). Excitation light was coupled to the microscope via a fiber optics light guide. A 425 nm dichroic mirror and a 500–530 nm bandpass emission filter were included in the light path. Fluorescence signals were measured with a photodiode (T.I.L.L. Photonics).

Fractional Ca^{2+} currents (P_f) were quantified using the relationship: P_f (%) = 100 * Q_{Ca}/Q_T, where Q_{Ca} is the charge carried by Ca^{2+} and Q_T is the total charge during a defined time interval. Q_T was derived as the total current integral and, in the case of GluR-$\delta2^{Lc}$ channels, included current through these channels as well as "leak" current. Q_{Ca} was derived from the relationship: $Q_{Ca} = \Delta F_{380}/f_{max}$, where ΔF_{380} is the change in the fluorescence signal with 380 nm excitation and f_{max} is the proportionality constant. To account for instabilities of the illumination intensity or the detection efficiency, ΔF_{380} was normalized to the fluorescence of beads (4.5-μm-diameter fluoresbrite BB beads; lot 481613; Polysciences, Warrington, PA) and expressed in "bead units" (BU) (Schneggenburger et al., 1993). The bead unit was determined on each experimental day as the mean fluorescence of 5–10 beads at 380 nm excitation. The proportionality constant f_{max} between the charge carried by inward Ca^{2+} and ΔF_{380} was determined at −100 mV in 10 mM Ca^{2+} and 140 mM NMDG using NMDA receptor (NMDAR) NR1–NR2A channels and was 0.04 ± 0.003 BU/pC ($n = 8$).

Leak current

Constitutively active GluR-$\delta2^{Lc}$ channels cannot be turned off because no intrinsic gating mechanism or any specific channel blockers have been identified. Therefore, the recording of current through Lurcher channels (I_{Lc}) cannot be distinguished from leak current (I_{leak}), and one records, under all experimental conditions, the total whole-cell current (I_T; $I_T = I_{Lc} + I_{leak}$). I_{leak} has two components: the current in the membrane of HEK 293 cells caused by endogenous channels ($I_{membrane}$ or I_m) and the current around the seal between the tip of the pipette and the cell (I_{seal} or I_s). Although both I_m and I_s could vary widely, I_s is more problematic because it can be extremely large. I_{leak} contaminates both current amplitudes and reversal potential measurements, complicating defining the properties of I_{Lc}. Because our objective was to characterize I_{Lc} but we could record only I_T, we characterized I_{leak} under our experimental conditions. Our goal here was twofold: (1) we wanted a criterion to determine when, relative to I_{Lc}, was I_{leak}, at least qualitatively, a significant component of I_T, and (2) we wanted an I_{leak} that represented "on average" the I_{leak} present during recordings of I_{Lc}.

To characterize I_{leak}, we recorded from HEK 293 cells that were either not transfected or were transfected with just GFP (both are referred to as "nontransfected"). We typically recorded from these nontransfected cells on the same day that recordings of I_{Lc} were made. Also, for both nontransfected and transfected cells, the seal resistance before entering into the whole-cell configuration was always at least 1 GΩ. (To increase the stability of whole-cell recordings, pipette tips were not fire-polished.) Nevertheless, despite our attempts to standardize recordings, we must emphasize that because GluR-$\delta2^{Lc}$ channels cannot be turned off, any definition of leak current during recordings of I_{Lc} can only be an average measure taken from a representative group of cells.

We recorded from a total of 16 nontransfected cells. Based on the current amplitudes at −100 mV in the high-Na^+ solution, the leak resistance (R_{leak}) ranged from 0.18 to 4.0 GΩ. Obviously, a lower leak resistance corresponds to a higher leak current, which would make characterizing I_{Lc} more difficult. We quantified a variety of parameters in these cells (e.g., the block by extracellular Ca^{2+}) and found that most showed no clear relationship to R_{leak}. However, one parameter did, namely, the change in the zero-current or reversal potential on replacing monovalents in the high-Na^+ solution with the large organic cation NMDG ($\Delta V_{rev,NMDG}$) (see Fig. 2A for an example recording). Indeed, R_{leak} showed a significantly ($p < 0.001$) strong correlation to $\Delta V_{rev,NMDG}$ ($R^2 = 0.76$; data not shown; the range of $\Delta V_{rev,NMDG}$ was from +0.3 to −55 mV). Hence, a more negative $\Delta V_{rev,NMDG}$ is, in general, indicative of a higher R_{leak} (that is, a smaller I_{leak}).

During recordings of Lurcher currents, the net reversal potential in NMDG is the weighted sum of the reversal potential for I_{leak} and I_{Lc}. NMDG is presumably only weakly permeable in Lurcher channels, as it is in all other GluR subtypes (Villarroel et al., 1995; Burnashev et al., 1996). Therefore, a more negative $\Delta V_{rev,NMDG}$ is not only consistent with a reduced leak current but also with a larger fraction of I_T being mediated by Lurcher channels. Therefore, concerning goal 1, we used $\Delta V_{rev,NMDG}$ as a qualitative index of the relative expression of Lurcher current to leak current with a more negative $\Delta V_{rev,NMDG}$ indicative, in general, of there being a larger fraction of Lurcher current. As a working cutoff, cells expressing Lurcher channels were included in the final analysis only when $\Delta V_{rev,NMDG}$ was more negative than −30 mV. This value was a compro-

mise between trying to maximize the fraction of the total current carried by Lurcher channels and getting a reasonable number of recordings. [With this criterion, for GluR-$\delta2^{Lc}$(Q), 12 out of 52 recordings were rejected, whereas for GluR-$\delta2^{Lc}$(R), 11 out of 30 recordings were rejected.] Also, this working cutoff had no qualitative effect on the results. For example, Ca^{2+}-dependent potentiation (see Fig. 3) was present in every cell expressing Lurcher channels regardless of $\Delta V_{rev,NMDG}$. In cells expressing GluR-$\delta2^{Lc}$(Q), when $\Delta V_{rev,NMDG}$ was more negative than −30 mV, G_{Ca}/G_{Na} for 2 mM Ca^{2+} was 2.4 ± 0.1 ($n = 17$), whereas when $\Delta V_{rev,NMDG}$ was more positive than −30 mV, G_{Ca}/G_{Na} was 1.8 ± 0.2 ($n = 8$). This reduced potentiation in cells in which $\Delta V_{rev,NMDG}$ was more positive than −30 mV is exactly what is expected if I_{leak} was a larger component of I_T.

Concerning goal 2, we distinguished the recordings of nontransfected cells into two groups, based in part on a natural break in R_{leak} as well as on their sharing similar properties.

Group I. In this group, $R_{leak} > 0.62$ GΩ ($n = 10$). The average R_{leak} was 1.3 ± 0.3 GΩ with a range of 0.62–3.9 GΩ. The average $\Delta V_{rev,NMDG}$ was −25 ± 5 mV. In addition, the overall shape of the current–voltage relationship was outwardly rectifying. Based on the ratio of the chord conductances at +100 mV (G_{+100}) to that at −100 mV (G_{-100}), the average rectification ratio G_{+100}/G_{-100} was 2.4 ± 0.2.

Group II. In this group, $R_{leak} < 500$ MΩ ($n = 6$). The average R_{leak} was 360 ± 50 MΩ with a range of 180–500 MΩ. The average $\Delta V_{rev,NMDG}$ was −8 ± 4 mV with an average rectification ratio of 1.6 ± 0.1.

We assumed that the on-average I_{leak} present during recordings of I_{Lc} was represented by Group I. We based this on the following: First, Group I recordings were indistinguishable from those of wild-type GluR-$\delta2$(Q) (see Figs. 2B,C, 3B). Second, for Group II recordings, current amplitudes, at −100 mV and in the high-Na^+ solution ($I_{amp} \sim$ −300 pA), were comparable with that in cells expressing GluR-$\delta2^{Lc}$(Q) ($I_{amp} \sim$ −300 pA) and considerably larger than that in cells expressing GluR-$\delta2^{Lc}$(R) ($I_{amp} \sim$ −200 pA). Yet on the basis of the results in Figures 2C and 3B it seems unlikely that nearly all of the current in cells transfected with GluR-$\delta2^{Lc}$(Q) is leak current.

RESULTS

Expression of Lurcher in HEK 293 cells

Figure 2 illustrates whole-cell currents produced by voltage ramps in HEK 293 cells expressing GluR-$\delta2$(Q), GluR-$\delta2^{Lc}$(Q), or GluR-$\delta2^{Lc}$(R). Cells were recorded either in the high-Na^+ solution (Fig. 2A, *solid lines*) or in a solution in which all monovalents were replaced by the large organic cation NMDG (*dashed lines*). For all three constructs, currents in the presence of NMDG, compared with those in high Na^+, reversed at more negative potentials and showed reduced amplitudes especially at negative potentials. In cells expressing GluR-$\delta2^{Lc}$(Q) and GluR-$\delta2^{Lc}$(R), currents differed from those expressing GluR-$\delta2$(Q) in two regards. First, current amplitudes, at −100 mV in the high-Na^+ solution, were consistently larger (Fig. 2B). Second, the chord conductance at −100 mV in high Na^+ relative to that in NMDG was significantly higher (Fig. 2C). For GluR-$\delta2$(Q), currents were indistinguishable from those in nontransfected cells under all experimental conditions.

These results are similar to those obtained for GluR-$\delta2$(Q) and GluR-$\delta2^{Lc}$(Q) expressed in *Xenopus* oocytes (Zuo et al., 1997) and are consistent with the Lurcher mutation inducing a constitutively active current. It should be noted that there is a quantitative difference between our measurements and those made previously (Zuo et al., 1997). This difference, however, reflects that the measurements in Figure 2 were made in the absence of any added Ca^{2+} that at physiological concentrations produced a strong potentiation of currents mediated by Lurcher channels (see Fig. 3).

Although reversal potentials in general were of little use in characterizing GluR-$\delta2^{Lc}$ current, we did use the change in the reversal potential after switching from high Na^+ to NMDG ($\Delta V_{rev,NMDG}$) as an index of the relative amount of Lurcher current to leak current (a more negative $\Delta V_{rev,NMDG}$ is indicative of a higher percentage of Lurcher current; see Materials and Methods). Cells expressing GluR-$\delta2^{Lc}$ were included in our analysis only when $\Delta V_{rev,NMDG}$ was more negative than −30 mV. In cells expressing GluR-$\delta2^{Lc}$(Q), $\Delta V_{rev,NMDG}$ was, on average, considerably more negative (−53 ± 2 mV; $n = 40$) than that in cells expressing GluR-$\delta2^{Lc}$(R) (−37 ± 1 mV; $n = 19$). Total currents in cells expressing GluR-$\delta2^{Lc}$(R) were also consistently smaller than those in cells expressing GluR-$\delta2^{Lc}$(Q) (Fig. 2B). $\Delta V_{rev,NMDG}$ is the weighted sum of the reversal potential of leak and Lurcher-

Figure 2. Expression of GluR-δ2(Q) and GluR-δ2^{Lc} in HEK 293 cells. *A*, Total whole-cell current at different membrane potentials in cells expressing GluR-δ2(Q), GluR-δ2^{Lc}(Q), or GluR-δ2^{Lc}(R). Currents were generated by voltage ramps (~120 mV·sec^{-1}) and were recorded in the high-Na$^+$ solution (*solid lines*) or in the same solution but with all of the monovalents replaced by NMDG (*dashed lines*). Both solutions contained 0.5 mM Mg^{2+} but no added Ca^{2+}. The internal solution contained 140 mM CsCl and 1 mM BAPTA. *B*, Peak current amplitudes, measured at −100 mV and in the high-Na$^+$ solution, from nontransfected cells (*non*) (Group I; see Materials and Methods) or from cells expressing GluR-δ2(Q), GluR-δ2^{Lc}(Q), or GluR-δ2^{Lc}(R). From *left* to *right*, the number of recordings was 10, 6, 40, and 19. Values shown, in this and all subsequent figures, are the mean ± 2 * SEM. The values for GluR-δ2^{Lc}(Q) and GluR-δ2^{Lc}(R) were statistically different from those for *non* and GluR-δ2(Q), as well as from each other. *C*, Chord conductance (*G*) ratio, at −100 mV, in high Na$^+$ (G_{Na}) relative to that in NMDG (G_{NMDG}). The averages are from the same cells shown in *B*. The values for GluR-δ2^{Lc}(Q) and GluR-δ2^{Lc}(R) were statistically different from those for *non* and GluR-δ2(Q) but were not significantly different from each other. For all expression constructs, we selected only cells fluorescent for GFP and assumed they also expressed the GluR subunit.
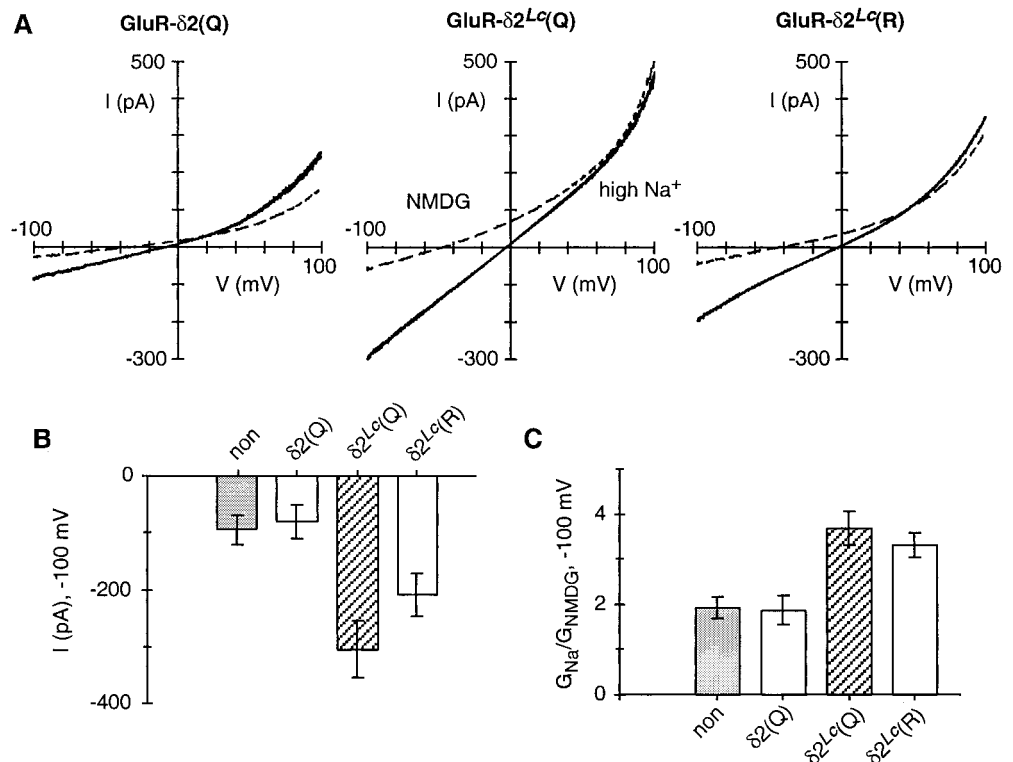
mediated currents. Hence assuming that the leak current is on average the same for cells expressing GluR-δ2^{Lc}(Q) or GluR-δ2^{Lc}(R) and that both channel types have the same low permeability to NMDG, then the less negative $\Delta V_{rev,NMDG}$ presumably reflects that leak current is a much larger fraction of the total current in cells expressing GluR-δ2^{Lc}(R).

Ca^{2+} potentiates currents mediated by GluR-δ2^{Lc} channels

Figure 3 illustrates the effect of Ca^{2+} at a physiological concentration on currents mediated by GluR-δ2^{Lc} channels. In Figure 3*A*, currents were recorded in the high-Na$^+$ solution (*solid lines*) or in the same solution but with added Ca^{2+} (2 mM; *dashed lines*). For GluR-δ2(Q), current amplitudes in the presence of Ca^{2+} were reduced over the entire voltage range. In contrast, current amplitudes in cells expressing GluR-δ2^{Lc}(Q) or GluR-δ2^{Lc}(R) were strongly enhanced. To quantify this potentiating effect, we measured the chord conductance, at −100 mV, in the presence (G_{Ca}) and absence (G_{Na}) of Ca^{2+} (Fig. 3*B*). For both nontransfected cells and cells expressing GluR-δ2(Q), the addition of Ca^{2+} always attenuated current amplitudes, resulting in a conductance ratio (G_{Ca}/G_{Na}) less than unity. In contrast, for GluR-δ2^{Lc}(Q) channels, G_{Ca}/G_{Na} was more than doubled (2.4 ± 0.1; *n* = 17), whereas for GluR-δ2^{Lc}(R) a similar effect of Ca^{2+} occurred, but the magnitude of the potentiation was smaller (1.8 ± 0.1; *n* = 7). This potentiation does not reflect intracellular changes of Ca^{2+}, because its magnitude was independent of the BAPTA concentration (0.1 or 10 mM) in the pipette (data not shown). Finally, this potentiation does not appear to be simply a diffuse, nonspecific electrostatic action of Ca^{2+} because it was unique for Ca^{2+}. Indeed, all other divalent ions tested either reduced (2 mM Ba^{2+}, Mg^{2+}, and Cd^{2+}; 0.87 ± 0.1; *n* = 3; 0.78 ± 0.1; *n* = 4; and 0.90 ± 0.05; *n* = 3, respectively) or had no effect (0.5 mM Zn^{2+}; 1.0 ± 0.05; *n* = 3) on current amplitudes.

To characterize this Ca^{2+}-dependent potentiation further, we measured its concentration dependence in GluR-δ2^{Lc}(Q). Potentiation was largest around physiological concentrations of Ca^{2+} (1 mM) and was reduced at both higher and lower concentrations (Fig. 3*C*). A fitted Hill equation to concentrations <2 mM (Fig. 3*C, solid line*) yielded a half-maximal response of ~300 μM Ca^{2+} and a Hill

coefficient of ~2. At higher concentrations, the reduction may reflect that Ca^{2+}, in addition to potentiating currents, is now also blocking current through GluR-δ2^{Lc}(Q) channels, an effect seen in other GluR subtypes (see Discussion).

To examine the kinetics and voltage dependence of the Ca^{2+}-dependent potentiation, we rapidly applied Ca^{2+} (2 mM) in high Na$^+$ to cells expressing GluR-δ2^{Lc}(Q) or GluR-δ2^{Lc}(R) at different membrane potentials (Fig. 4). As illustrated in Figure 4*A*, the addition of Ca^{2+}, in this case at −60 mV, induced a slowly developing inward current for both GluR-δ2^{Lc}(Q) and GluR-δ2^{Lc}(R). The time course for this process was typically well described by a single exponential. The average exponential time constants (τs) over a wide voltage range are shown in Figure 4*B* for GluR-δ2^{Lc}(Q) (*open circles*) and GluR-δ2^{Lc}(R) (*solid circles*). The τs over the entire voltage range were indistinguisable for GluR-δ2^{Lc}(Q) and GluR-δ2^{Lc}(R) and independent of voltage, suggesting that the site mediating this Ca^{2+}-dependent potentiation is not within the transmembrane electric field.

In summary, current through GluR-δ2^{Lc} channels shows a robust Ca^{2+}-dependent potentiation. The maximal potentiation occurs around physiological concentrations of Ca^{2+}. The site of action for Ca^{2+} is on the external face of the protein, as suggested by the lack of voltage dependence for the potentiation and its insensitivity to intracellular BAPTA. The degree of potentiation is larger in GluR-δ2^{Lc}(Q) than in GluR-δ2^{Lc}(R) (Fig. 3*B*). Nevertheless, this difference may reflect that the current amplitudes for GluR-δ2^{Lc}(R) are smaller than those for GluR-δ2^{Lc}(Q) [i.e., potentiation in GluR-δ2^{Lc}(R) may be reduced simply because more of the total current is being carried by the leak current]. In support of this idea, the time course—which is independent of the total amount of GluR-δ2^{Lc} channels in the cell—showed no difference between GluR-δ2^{Lc}(Q) and GluR-δ2^{Lc}(R) channels. Thus, this Ca^{2+}-dependent potentiation appears to be independent of ion fluxes and may reflect a gating-induced conformational change in the protein.

Currents mediated by GluR-δ2^{Lc}(Q) but not by GluR-δ2^{Lc}(R) are doubly rectifying

Ca^{2+}-permeable AMPA/kainate receptor channels show a doubly rectifying current–voltage relationship caused by a voltage-dependent block by intracellular polyamines (Bowie and Mayer,
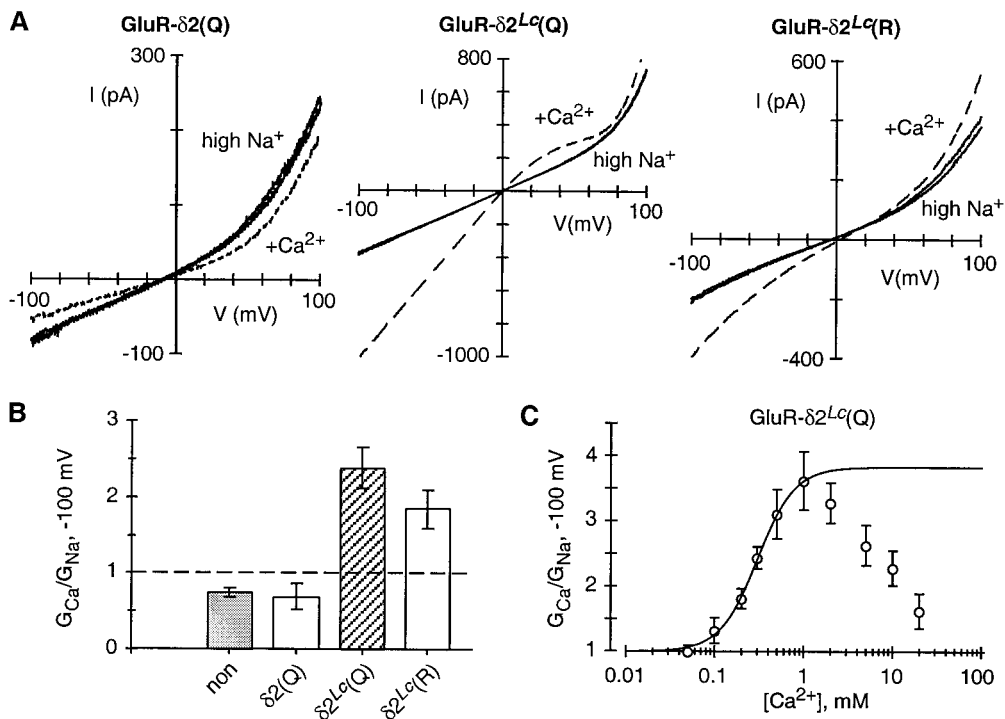
Figure 3. Extracellular Ca^{2+} potentiates current through GluR-$\delta 2^{Lc}$ channels. *A*, Total whole-cell currents at different membrane potentials in cells expressing GluR-$\delta 2$(Q), GluR-$\delta 2^{Lc}$(Q), or GluR-$\delta 2^{Lc}$(R). Currents were generated and displayed as described in Figure 2*A* except that cells were recorded in the high-Na^+ solution (*solid lines*) or in the same solution but with added Ca^{2+} (2 mM; *dashed lines*). *B*, Chord conductance ratio, at −100 mV, in the presence of added Ca^{2+} (G_{Ca}) relative to that in the same solution but without added Ca^{2+} (the high-Na^+ solution; G_{Na}). From *left* to *right*, the number of recordings was 10, 6, 17, and 7. The values for GluR-$\delta 2^{Lc}$(Q) and GluR-$\delta 2^{Lc}$(R) were statistically different from those for *non* and GluR-$\delta 2$(Q), as well as from each other. *C*, Concentration dependence of the Ca^{2+}-induced potentiation in GluR-$\delta 2^{Lc}$(Q) channels. The *solid line* through the *points* at concentrations <2 mM is a fitted Hill equation [= $G_{max}/(1 + (K_{0.5}/[Ca^{2+}])^n)$], where G_{max} is the maximal conductance (G_{Ca}/G_{Na}), $K_{0.5}$ is the Ca^{2+} concentration corresponding to the half-maximal response, and n is the Hill coefficient. This fit yielded a G_{max} of ~3.0, a $K_{0.5}$ of ~300 μM, and a Hill coefficient of ~2. A minimum of five recordings was made at each concentration.
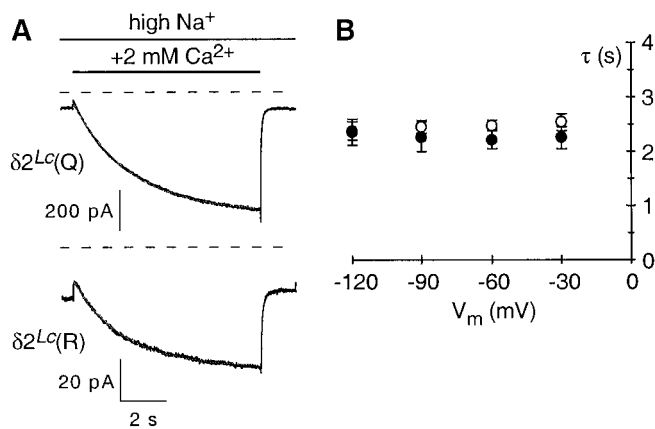
1995; Koh et al., 1995). This double rectification shows a characteristic shape, with the block occurring primarily at positive potentials, and is lost in channels when the positively charged arginine occupies the Q/R site. GluR-$\delta 2^{Lc}$(Q) channels show a clear double rectification in the presence of Ca^{2+} (Fig. 3*A*). In the absence of Ca^{2+}, however, any double rectification is less obvious. In part this may reflect that in the presence of Ca^{2+} the signal-to-noise ratio is greatly enhanced (current through GluR-$\delta 2^{Lc}$ channels is potentiated, and the leak current is reduced in amplitude). Therefore, to compare the overall shape of the current–voltage relationship under different conditions, we subtracted off the on-average leak

Figure 4. Time course of Ca^{2+}-induced potentiation. *A*, Rapid application of Ca^{2+} to cells expressing GluR-$\delta 2^{Lc}$(Q) (*top*) or GluR-$\delta 2^{Lc}$(R) (*bottom*). The cells were continuously bathed in the high-Na^+ solution, and during the time indicated by the *solid bar*, 2 mM Ca^{2+} (in the high-Na^+ solution) was rapidly applied (8 sec duration). The exchange time of the open tip response was <2 msec. The *dashed lines* indicate the respective zero-current levels. The holding potential was −60 mV. Note that after removal of Ca^{2+}, the current amplitudes rapidly returned to the baseline level. The offset in the current amplitudes during the initial phase of Ca^{2+} application is caused, in part, by Ca^{2+} block of the leak current. *B*, Voltage dependence of the time course for the development of Ca^{2+}-induced potentiation. Average exponential time constants (τs) were derived from the single-exponential fits of responses shown in *A*. A minimum of three recordings were made at each potential (−120, −90, −60, and −30 mV) for GluR-$\delta 2^{Lc}$(Q) (*open circles*) and GluR-$\delta 2^{Lc}$(R) (*solid circles*).

current (Group I; see Materials and Methods) from the average current of the recordings shown in Figure 3, *A* and *B*. We assumed in this analysis that the on-average leak current was the same for cells expressing GluR-$\delta 2^{Lc}$(Q) or GluR-$\delta 2^{Lc}$(R).
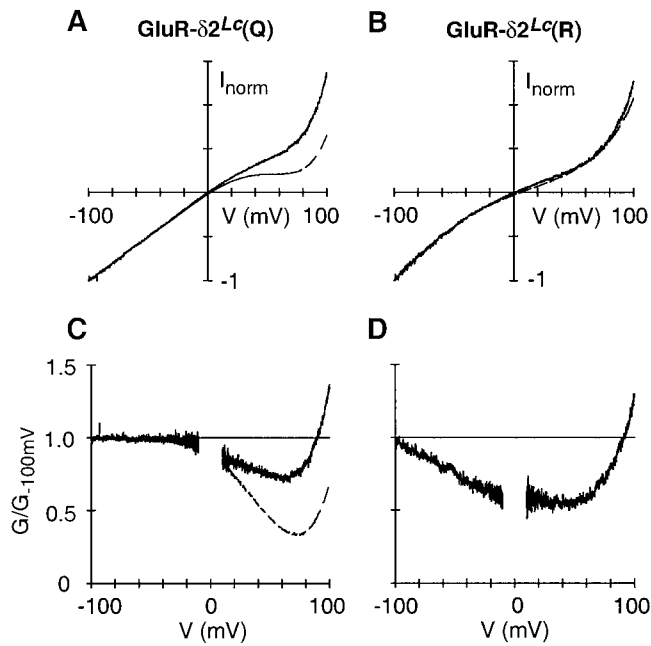
Figure 5, *A* and *B*, shows the average leak-subtracted currents, normalized to the current amplitude at −100 mV, for cells expressing either GluR-$\delta 2^{Lc}$(Q) or GluR-$\delta 2^{Lc}$(R). Currents were recorded either in the presence (*dashed line*) or absence (*solid line*) of Ca^{2+}. In the case of GluR-$\delta 2^{Lc}$(Q) (Fig. 5*A*), a clear double rectification is present in both the presence and absence of Ca^{2+}, but a difference in the magnitude of this rectification is evident. To examine the rectification further, we plotted the conductance relative to the conductance at −100 mV (Fig. 5*C*), in a manner similar to that done previously for AMPA/kainate channels (Bowie and Mayer, 1995). In the presence of Ca^{2+}, the normalized conductance plot showed a large region of non-uniform conductance at potentials positive to ~0 mV, whereas in the absence of Ca^{2+} (Fig. 5*C*, *noisier trace*), this negative region still exists but is reduced in magnitude. Thus, GluR-$\delta 2^{Lc}$(Q) channels display the double rectification typical of Ca^{2+}-permeable AMPA/kainate receptor channels and therefore are likely to be blocked by intracellular polyamines. The difference in the degree of potentiation may reflect that the conformational change associated with Ca^{2+} potentiation yields channels with a higher affinity for polyamines. In addition, if this rectification is caused by block by intracellular polyamines, then GluR-$\delta 2^{Lc}$(Q) channels have a low affinity for polyamines.

Average currents in GluR-$\delta 2^{Lc}$(R) (Fig. 5*B,D*) showed two significant differences from those in GluR-$\delta 2^{Lc}$(Q). First, normalized current amplitudes, in the presence and absence of Ca^{2+}, were essentially indistinguishable for GluR-$\delta 2^{Lc}$(R) over the entire voltage range, indicating that the potentiation in Ca^{2+} is just a scaled-up record of the current amplitudes in the absence of Ca^{2+}. Second, although the current–voltage relation does show rectification, it is distinct from the double rectification associated with polyamine block being manifested as an inward rectification at extremely negative potentials and an outward rectification at extremely positive potentials (Fig. 5*B*).

In summary, GluR-$\delta 2^{Lc}$(Q) channels show double rectification, a characteristic feature of Ca^{2+}-permeable AMPA/kainate GluR channels. Furthermore, as in AMPA/kainate channels, the pres-

Figure 5. Overall shape of the current–voltage relation. *A, B,* On-average leak-subtracted current amplitudes in cells expressing GluR-δ2^{Lc}(Q) (*A*) or GluR-δ2^{Lc}(R) (*B*). The on-average leak current (Group I) was subtracted off of the average current amplitudes of cells expressing GluR-δ2^{Lc}(Q) (*n* = 17) or GluR-δ2^{Lc}(R) (*n* = 7) (same cells shown in Fig. 3*A,B*). Cells were bathed in the high-Na$^+$ solution (*solid lines*) or in the same solution but with added Ca^{2+} (2 mM; *dashed lines*). For comparison, current amplitudes were normalized (*norm*) to the current amplitude at −100 mV. *C, D,* Ratio of the chord conductance, in Na$^+$ or in Ca^{2+}, divided by the respective chord conductance at −100 mV (G_{-100}) in cells expressing GluR-δ2^{Lc}(Q) (*C*) or GluR-δ2^{Lc}(R) (*D*). The *noisier trace* is the high-Na$^+$ *trace*. For *D*, only the high-Na$^+$ *trace* is shown. For clarity, the ratio was removed at potentials ± 10 mV of 0 mV.

ence of the positively charged arginine at the Q/R site removes the double rectification typical of polyamine block.

GluR-δ2^{Lc}(Q) channels are permeable to Ca^{2+}

AMPA/kainate receptors blocked by intracellular polyamines are also Ca^{2+} permeable. To test whether this is also true for Lurcher channels, we measured changes in the reversal potential on switching from a Ca^{2+}-free to a Ca^{2+}-containing solution. For cells expressing GluR-δ2^{Lc}(Q) or GluR-δ2^{Lc}(R), reversal potentials, when switching from high Na$^+$ to high Na$^+$ plus Ca^{2+} (2 or 20 mM), were shifted positive, but the magnitude of this shift was comparable with that in nontransfected cells (data not shown). Thus, changes in reversal potentials especially under physiological conditions are inconclusive about Ca^{2+} permeability in GluR-δ2^{Lc} channels.

We took an alternative approach to quantifying Ca^{2+} permeability in GluR-δ2^{Lc} channels by simultaneously measuring whole-cell currents and changes in fura-2 fluorescence with 380 nm excitation. The analysis of such an experiment yields the fraction of the total current carried by Ca^{2+}. This quantity, termed fractional Ca^{2+} current, is the most accurate description of Ca^{2+} permeation in channels having a mixed monovalent/Ca^{2+} permeability under physiological conditions (Schneggenburger et al., 1993; Neher, 1995). To circumvent the problem of Ca^{2+} entry during baseline measurements, we rapidly applied the Ca^{2+}-containing solution to expose cells transiently to Ca^{2+}.

Figure 6 illustrates our approach to quantifying fractional Ca^{2+} currents in Lurcher channels. We continuously bathed cells in the high-Na$^+$ solution and then, during the time indicated by the *solid bar* (Fig. 6), rapidly applied the same solution but with added Ca^{2+} (2 mM). The addition of Ca^{2+} either reduced current amplitudes [GluR-δ2(Q) as well as nontransfected cells] or induced a slow potentiation [GluR-δ2^{Lc}(Q) and GluR-δ2^{Lc}(R)]. Similarly, it elic-
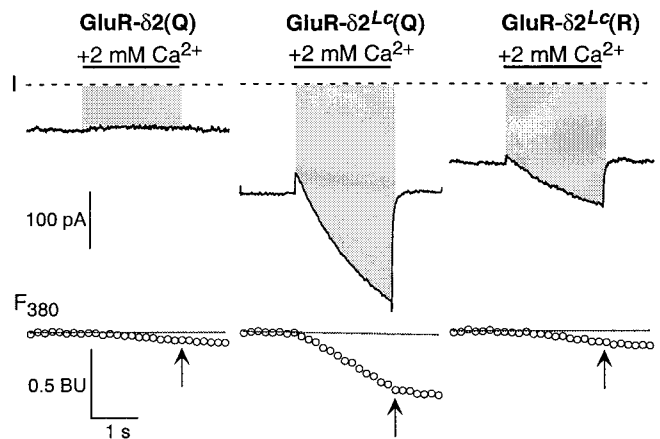

Figure 6. Measurement of Ca^{2+} influx in GluR-δ2^{Lc} channels. Simultaneous measurement of total whole-cell current (*I; top*) and fluorescent intensity with 380 nm excitation (F_{380}; *bottom*). The recordings are from cells expressing GluR-δ2(Q), GluR-δ2^{Lc}(Q), or GluR-δ2^{Lc}(R). Cells were continuously bathed in the high-Na$^+$ solution and, during the time indicated by the *solid bar*, exposed to 2 mM Ca^{2+} (2 sec duration). The pipette solution contained 140 mM CsCl and 1 mM fura-2. The *dashed lines* in the *current plots* reflect the zero-current level. The corresponding F_{380}, expressed in BU, is shown *below* as *open symbols*. The *arrows* in the F_{380} traces indicate the time point at which the current integral (Q_T) and ΔF_{380} were quantified. The *shaded region*, extending from the whole-cell current to the zero-current line, defined Q_T. Hence, for GluR-δ2^{Lc}, Q_T is the current integral for current through these channels as well as the leak current. ΔF_{380} was taken as the difference between the F_{380} amplitude at the *arrow* and the baseline F_{380} signal (*solid line*) that was extrapolated from a linear fit to the F_{380} amplitudes before the Ca^{2+} application. The holding potential was −60 mV.

ited a change in F_{380}, the magnitude of which depended strongly on the construct expressed by the cell. In the case of cells transfected with GluR-δ2(Q) or nontransfected cells, this ΔF_{380} was small but nonzero and presumably reflects Ca^{2+} influx as part of the leak current. Similarly, ΔF_{380} was small in GluR-δ2^{Lc}(R), whereas in GluR-δ2^{Lc}(Q) it was considerably larger. This ΔF_{380} was used to calculate the charge carried by Ca^{2+} (Q_{Ca}; $Q_{Ca} = \Delta F_{380}/f_{max}$) during the defined time intervals (Fig. 6, *arrows*). During the same interval, we quantified the current integral (Q_T) that in the case of GluR-δ2^{Lc} channels encompasses both current through Lurcher channels as well as the leak current.

Although the largest ΔF_{380} was seen in GluR-δ2^{Lc}(Q) channels, they also showed the largest current integrals. We therefore compared the charge carried by Ca^{2+} per unit total charge (Q_{Ca}/Q_T) across the different conditions (Fig. 7*A*). Q_{Ca}/Q_T normalizes for the differences in the magnitude of the total current. It was significantly higher for GluR-δ2^{Lc}(Q) than for GluR-δ2^{Lc}(R) as well as for nontransfected cells and cells expressing GluR-δ2(Q) [non/δ2(Q)]. There was also a trend for Q_{Ca}/Q_T to be lowest in GluR-δ2^{Lc}(R), presumably reflecting that although Q_{Ca} differed little from that in non/δ2(Q), the current integral was considerably larger. These results, which are independent of any correction of the data, demonstrate that GluR-δ2^{Lc}(Q) channels facilitate Ca^{2+} influx and that the substitution of the positively charged arginine at the Q/R site attenuates this process.

Figure 7*B* shows fractional Ca^{2+} currents for the GluR subtypes, including GluR-δ2^{Lc}(Q) and GluR-δ2^{Lc}(R). To obtain values in which the contribution of the leak current was minimized, we subtracted off the average Q_{Ca} and Q_T recorded for nontransfected cells and cells transfected with GluR-δ2(Q) from the average Q_{Ca} and Q_T for cells expressing GluR-δ2^{Lc}(Q) or GluR-δ2^{Lc}(R) ($P_f = 100 * Q_{Ca}/Q_T$). With this approach, GluR-δ2^{Lc}(Q) channels show an apparent fractional Ca^{2+} current (2.6 ± 0.6) comparable with that found in AMPA/kainate receptor channels. In addition, in GluR-δ2^{Lc}(R), the apparent P_f was strongly reduced (0.3 ± 0.3), suggesting that these channels are essentially impermeable to Ca^{2+}.
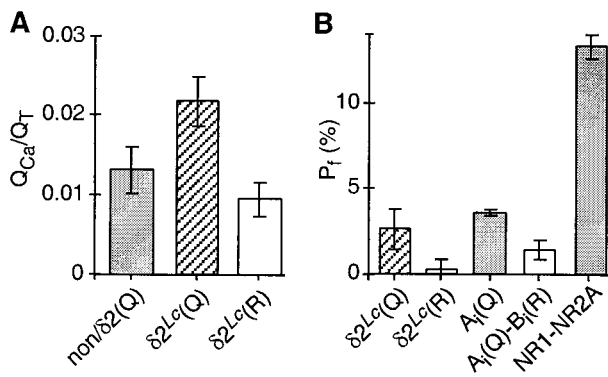
Figure 7. Fractional Ca^{2+} currents in GluR-$\delta2^{Lc}$ channels. *A*, Ratio of the charge carried by Ca^{2+} (Q_{Ca}) to the total charge (Q_T) in nontransfected cells or cells transfected with GluR-$\delta2$ [*non/$\delta2(Q)$*] or in cells expressing GluR-$\delta2^{Lc}(Q)$ or GluR-$\delta2^{Lc}(R)$. Q_{Ca} was derived from the relationship: $Q_{Ca} = \Delta F_{380}/f_{max}$, where $f_{max} = 0.04 \pm 0.003$ BU/pC. Q_T was derived from the current integral (Fig. 6, *shaded regions*). The number of recordings was, from *left* to *right*, 14, 10, and 12. *B*, Fractional Ca^{2+} currents in GluR subtypes. For GluR-$\delta2^{Lc}$ channels, the average Q_{Ca} and Q_T, obtained for nontransfected cells and cells transfected with GluR-$\delta2(Q)$, were subtracted off of the respective average parameters for GluR-$\delta2^{Lc}(Q)$ and GluR-$\delta2^{Lc}(R)$. The derived P_f values were 2.6 ± 0.6 [GluR-$\delta2^{Lc}(Q)$] and 0.3 ± 0.3 [GluR-$\delta2^{Lc}(R)$]. The values for GluR-A(Q) and NR1-NR2A are from Wollmuth and Sakmann (1998), whereas those for the A(Q)–B(R) mixture (transfected at a ratio of 4:1) are unpublished (L. P. Wollmuth, unpublished observations) but are comparable with those published previously (Burnashev et al., 1995).

DISCUSSION

Neurodegeneration in Lurcher mice has been traced by positional cloning to the GluR-$\delta2$ channel (Zuo et al., 1997), an orphan member of the ionotropic GluR family. A single amino acid substitution in the highly conserved M3 segment of GluR-$\delta2$ renders these channels constitutively active. This finding provided not only a molecular basis for the selective loss of Purkinje neurons in Lurcher mice but also a means to study the GluR-$\delta2$ subunit. We exploited this constitutive activation to characterize the basic properties of ion permeation in these receptor channels.

Assumptions and technical challenges of our approach

In the absence of any specific ligand, constitutive activation provides the only means to study ion permeation in GluR-$\delta2$ channels. However, measuring current through constitutively active channels involves numerous practical problems. The most pressing is that the contribution of the leak current to the total current cannot be properly defined. This is especially problematic in the absence of Ca^{2+} when leak current is on the same order of magnitude as the presumed current mediated by Lurcher channels. We therefore used several approaches to help define Lurcher current and to minimize the contribution of leak current to our recordings. First, as done previously (Zuo et al., 1997), we used NMDG as a means to test for Lurcher current. In cells transfected with GluR-$\delta2^{Lc}$, the conductance in Na^+ relative to that in NMDG was significantly greater than that in cells transfected with GluR-$\delta2(Q)$ (Fig. 2), indicating that a significant component of the total current measured in cells transfected with GluR-$\delta2^{Lc}$ is mediated by these channels. Second, we found that the change in the reversal potential on exchanging the high-Na^+ with the NMDG solution was a good index, at least qualitatively, of the relative amount of Lurcher and leak current within a cell and did not include recordings in our final analysis when the change in the reversal potential was more positive than -30 mV (see Materials and Methods for a further discussion). Finally, we defined an on-average leak current that we assumed represented the leak current during recordings of Lurcher channels.

The pore properties of GluR-$\delta2^{Lc}$ are similar to those of AMPA/kainate receptor channels

In terms of the entire protein, but especially in terms of those residues that form the core of the ion channel, GluR-$\delta2$ shows a

much higher sequence similarity to AMPA/kainate than to NMDA receptor channels (Fig. 1). We found that the pore of GluR-$\delta2^{Lc}$ also shows functional similarities to Ca^{2+}-permeable AMPA/kainate receptor channels. Indeed, current through GluR-$\delta2^{Lc}(Q)$ channels shows a doubly rectifying current–voltage relationship typical of the block by intracellular polyamines of Ca^{2+}-permeable AMPA/kainate receptor channels (Bowie and Mayer, 1995; Koh et al., 1995). Similarly, GluR-$\delta2^{Lc}(Q)$ channels show a moderate fractional Ca^{2+} current (~2–3%), comparable in magnitude with that found in Ca^{2+}-permeable AMPA/kainate channels (~1–3% for kainate and ~3–5% for AMPAR compared with ~14% for NMDAR channels) (Burnashev et al., 1995; Wollmuth and Sakmann, 1998). Like in AMPA/kainate receptor channels, both the double rectification and moderate Ca^{2+} permeability are significantly attenuated in channels where the positively charged arginine occupies the Q/R site in GluR-$\delta2^{Lc}$ [GluR-$\delta2^{Lc}(R)$].

Although Lurcher channels share properties with kainate/AMPA receptor channels, there are also important differences. For example, neither kainate nor AMPA receptor channels show an increased double rectification in the presence of Ca^{2+} (which we assume to reflect an increase in affinity for polyamines). Also, the presumed polyamine block, even in the presence of Ca^{2+} (Fig. 5A), is much weaker than that found in non-NMDA channels (cf. Bowie and Mayer, 1995). Finally, as discussed below, no GluR subtype shows a potentiation by Ca^{2+}.

A critical question concerning the mechanism of Lurcher-mediated signal transduction is whether it forms an ion channel or acts as an accessory protein regulating the activity of other channels in the membrane- or cytoplasmic-signaling cascades. The evidence that an arginine residue at the Q/R site defines Ca^{2+} permeation and blocking properties in Lurcher subunits indicates that GluR-$\delta2^{Lc}$ indeed forms ion channels. Further support of this idea arises from the observation that GluR-$\delta2^{Lc}$ shows comparable properties in cerebellar Purkinje neurons and two heterologous expression systems, *Xenopus* oocytes and HEK 293 cells. Thus, the constitutive current associated with Lurcher is mediated directly by the channels it forms. The possibility still remains, however, that Lurcher or wild-type GluR-$\delta2$ interacts with other proteins involved in cytoplasmic signaling.

We assume that the permeation properties found for GluR-$\delta2^{Lc}$ reflect those of the channel formed by wild-type GluR-$\delta2$. However, the Lurcher mutation, which occurs at a channel-lining position (Beck et al., 1999), may have direct effects on ion permeation. Indeed, substitutions of an asparagine residue located three positions N-terminal to the Lurcher position in the NMDAR NR1 subunit alters Ca^{2+} permeability (Beck et al., 1999). Nevertheless, substitutions of sites in the extracellular vestibule affect Ca^{2+} permeation only moderately, and it seems unlikely that the alanine to threonine substitution would significantly alter the Ca^{2+} permeability properties of Lurcher channels.

Ca^{2+}-dependent potentiation

Lurcher channels are potentiated by extracellular Ca^{2+} at physiological concentrations (Fig. 3). This Ca^{2+}-dependent potentiation is not found in any other subtype of GluR channel. Rather, physiological concentrations of Ca^{2+} are found to block the monovalent current through NMDA (Ascher and Nowak, 1988), kainate (Gu and Huang, 1991), and AMPA (C. Jatzke and L. P. Wollmuth, unpublished observations) receptor channels. Extracellular Ca^{2+} can potentiate current through NMDAR channels via a change in the affinity for glycine, but this effect occurs only at high concentrations of Ca^{2+} (10 mM) (Gu and Huang, 1994).

The molecular basis for this potentiation in Lurcher channels is unknown but appears to arise via an extracellular action of Ca^{2+}. It also seems specific for Ca^{2+} because all other divalent cations tested reduced current amplitudes. One possibility is that Lurcher channels in the absence of Ca^{2+} are in a low-conducting state and that Ca^{2+} acts as a ligand to shift them to a higher-conducting state. That some conformational change is associated with the transition to the Ca^{2+}-potentiated state is indicated by an appar-

ently higher affinity for intracellular polyamines (Fig. 5). Nevertheless, the process underlying the Ca^{2+}-dependent potentiation remains unknown. Also, although this Ca^{2+}-dependent potentiation could be highly significant in terms of the Lurcher phenotype and the function of GluR-δ2 (see below), it remains unclear whether this property is found in wild-type GluR-δ2 channels because the Lurcher mutation is associated with a change in the gating properties of the channel.

Physiological consequences of Ca^{2+} interaction with Lurcher channels

Ca^{2+} interacts with GluR-$\delta 2^{Lc}$(Q) channels in two interesting regards. It shows a moderate permeability through the channels, and it potentiates current through them. Both of these processes could directly or indirectly contribute to the cell death associated with the Lurcher mutation. Indeed, Ca^{2+} influx via GluRs has been proposed to contribute to excitotoxic cell death (Choi, 1994). In addition, extracellular Ca^{2+} may potentiate the current mediated by Lurcher channels in Purkinje neurons, further disrupting the resting membrane potential. Nevertheless, the contribution of either or both of these processes to the cell death associated with the Lurcher mutation remains unknown.

Structural conservation and function of the M3 segment

The M3 segment is the most highly conserved segment among GluRs. This is especially true for the SYTANLAAF motif where the Lurcher mutation lies (Zuo et al., 1997) (see Fig. 1). The functional effects of the Lurcher mutation suggest a role of this segment in channel gating. The ubiquitous nature of this motif in GluR channel function is seen by the fact that, as in GluR-δ2, the introduction of the Lurcher mutation in a *Caenorhabditis elegans* glutamate receptor, GLR-1, led to constitutively active channels (Zheng et al., 1999). In addition, covalent modification of a cysteine substituted at the adjacent alanine in the NMDAR NR1 subunit results in a constitutively open channel (Beck et al., 1999). Unknown, however, is the mechanism by which the Lurcher mutation alters the gating properties of GluR channels.

Function of wild-type GluR-δ2 in Purkinje neurons

The cellular function of GluR-δ2 remains unclear. Our results, although indirect, suggest some alternatives. Clearly, Lurcher subunits and therefore presumably the wild-type GluR-δ2 can form ion channels with permeation properties like those of Ca^{2+}-permeable AMPA/kainate receptor channels. Wild-type GluR-δ2 may therefore form channels by itself or in combination with other GluR subunits *in vivo*. Such channels, if formed with other subunits, could display altered Ca^{2+} permeability properties, block by intracellular polyamines, and/or Ca^{2+}-dependent potentiation. Although no direct evidence exists for GluR-δ2 forming channel complexes with other GluR subtypes, GluR-δ2 is concentrated at the postsynaptic specialization, not in the extrasynaptic membrane, and colocalized with AMPA and NMDA receptors (Takumi et al., 1999).

Although mice lacking GluR-δ2 display defects in cerebellar long-term depression (LTD), exactly how GluR-δ2 is involved in this process is unknown (Linden, 1994; Kashiwabuchi et al., 1995). Either Ca^{2+} influx or Ca^{2+}-dependent potentiation could contribute to the role of GluR-δ2 in cerebellar LTD. Because the site mediating Ca^{2+}-dependent potentiation appears extracellular and distinct from the pore-forming domains, wild-type GluR-δ2 could have the same capability to switch from a low-conducting to a high-conducting state after binding to extracellular Ca^{2+} as that observed for the Lurcher channel.

REFERENCES

Araki K, Meguro H, Kushiya E, Takayama C, Inoue Y, Mishina M (1993) Selective expression of the glutamate receptor channel delta 2 subunit in cerebellar Purkinje cells. Biochem Biophys Res Commun 197:1267–1276.
Ascher P, Nowak L (1988) The role of divalent cations in the *N*-methyl-

D-aspartate responses of mouse central neurones in culture. J Physiol (Lond) 399:247–266.
Beck C, Wollmuth LP, Seeburg PH, Sakmann B, Kuner T (1999) NMDAR channel segments forming the extracellular vestibule inferred from the accessibility of substituted cysteines. Neuron 22:559–570.
Bowie D, Mayer ML (1995) Inward rectification of both AMPA and kainate subtype glutamate receptors generated by polyamine-mediated ion channel block. Neuron 15:453–462.
Burnashev N (1996) Calcium permeability of glutamate-gated channels in the central nervous system. Curr Opin Neurobiol 6:311–317.
Burnashev N, Zhou Z, Neher E, Sakmann B (1995) Fractional calcium currents through recombinant GluR channels of the NMDA, AMPA and kainate receptor subtypes. J Physiol (Lond) 485:403–418.
Burnashev N, Villarroel A, Sakmann B (1996) Dimensions and ion selectivity of recombinant AMPA and kainate receptor channels and their dependence on Q/R site residues. J Physiol (Lond) 496:165–173.
Choi DW (1994) Glutamate receptors and the induction of excitotoxic neuronal death. Prog Brain Res 100:47–51.
Gu Y, Huang L-TM (1991) Block of kainate receptor channels by Ca^{2+} in isolated spinal trigeminal neurons of rat. Neuron 6:777–784.
Gu Y, Huang LY (1994) Modulation of glycine affinity for NMDA receptors by extracellular Ca^{2+} in trigeminal neurons. J Neurosci 14:4561–4570.
Heintz N, De Jager PL (1999) GluR delta 2 and the development and death of cerebellar Purkinje neurons in lurcher mice. Ann N Y Acad Sci 868:502–514.
Ho SN, Hunt HD, Horton RM, Pullen JK, Pease LR (1989) Site-directed mutagenesis by overlap extension using the polymerase chain reaction. Gene 77:51–59.
Kashiwabuchi N, Ikeda K, Araki K, Hirano T, Shibuki K, Takayama C, Inoue Y, Kutsuwada T, Yagi T, Kang Y, Aizawa S, Mishina M (1995) Impairment of motor coordination, Purkinje cell synapse formation, and cerebellar long-term depression in GluR delta 2 mutant mice. Cell 81:245–252.
Koh D-S, Burnashev N, Jonas P (1995) Block of native Ca^{2+}-permeable AMPA receptors in rat brain by intracellular polyamines generates double rectification. J Physiol (Lond) 486:305–312.
Kuner T, Wollmuth LP, Sakmann B (1999) The ion-conducting pore of glutamate receptor channels. In: Ionotropic glutamate receptors in the CNS, Vol 141 (Jonas P, Monyer H, eds), pp 219–249. Berlin: Springer.
Landsend AS, Amiry-Moghaddam M, Matsubara A, Bergersen L, Usami S, Wenthold RJ, Ottersen OP (1997) Differential localization of δ glutamate receptors in the rat cerebellum: coexpression with AMPA receptors in parallel fiber→spine synapses and absence from climbing fiber→spine synapses. J Neurosci 17:834–842.
Linden DJ (1994) Long-term synaptic depression in the mammalian brain. Neuron 12:457–472.
Lomeli H, Sprengel R, Laurie DJ, Kohr G, Herb A, Seeburg PH, Wisden W (1993) The rat delta-1 and delta-2 subunits extend the excitatory amino acid receptor family. FEBS Lett 315:318–322.
Neher E (1995) The use of fura-2 for estimating Ca buffers and Ca fluxes. Neuropharmacology 34:1423–1442.
Schneggenburger R, Zhou Z, Konnerth A, Neher E (1993) Fractional contribution of calcium to the cation current through glutamate receptor channels. Neuron 11:133–143.
Seeburg PH (1993) The molecular biology of mammalian glutamate receptor channels. Trends Neurosci 16:359–365.
Takumi Y, Matsubara A, Rinvik E, Ottersen OP (1999) The arrangement of glutamate receptors in excitatory synapses. Ann N Y Acad Sci 868:474–482.
Villarroel A, Burnashev N, Sakmann B (1995) Dimensions of the narrow portion of a recombinant NMDA receptor channel. Biophys J 68:866–875.
Wollmuth LP, Sakmann B (1998) Different mechanisms of Ca^{2+} transport in NMDA and Ca^{2+}-permeable AMPA glutamate receptor channels. J Gen Physiol 112:623–636.
Wollmuth LP, Kuner T, Seeburg PH, Sakmann B (1996) Differential contribution of the NR1- and NR2A-subunits to the selectivity filter of recombinant NMDA receptor channels. J Physiol (Lond) 491:779–797.
Yamazaki M, Araki K, Shibata A, Mishina M (1992) Molecular cloning of a cDNA encoding a novel member of the mouse glutamate receptor channel family. Biochem Biophys Res Commun 183:886–892.
Zhao HM, Wenthold RJ, Wang YX, Petralia RS (1997) Delta-glutamate receptors are differentially distributed at parallel and climbing fiber synapses on Purkinje cells. J Neurochem 68:1041–1052.
Zheng Y, Brockie PJ, Mellem JE, Madsen DM, Maricq AV (1999) Neuronal control of locomotion in *C. elegans* is modified by a dominant mutation in the GLR-1 ionotropic glutamate receptor. Neuron 24:347–361.
Zuo J, De Jager PL, Takahashi KA, Jiang W, Linden DJ, Heintz N (1997) Neurodegeneration in Lurcher mice caused by mutation in delta2 glutamate receptor gene. Nature 388:769–773.